

# Radiation properties of extreme nulling pulsar J1502–5653

J. Li<sup>1,2</sup>, A. Esamdin<sup>1\*</sup>, R. N. Manchester<sup>3</sup>, M. F. Qian<sup>1,2</sup>, H. B. Niu<sup>1,2</sup>

<sup>1</sup>*Xinjiang Astronomical Observatory, Chinese Academy of Sciences, 150, Science 1-street, Urumqi, Xinjiang, 830011, China*

<sup>2</sup>*Graduate University of Chinese Academy of Sciences, 19A Yuquan Road, Beijing, 100049, China*

<sup>3</sup>*CSIRO Astronomy and Space Science, Australia Telescope National Facility, PO Box 76, Epping NSW 1710, Australia*

10 September 2018

## ABSTRACT

We report on radiation properties of extreme nulling pulsar J1502–5653, by analyzing the data acquired from the Parkes 64-m telescope at 1374 MHz. The radio emission from this pulsar exhibits sequences of several tens to several hundreds consecutive burst pulses, separated by null pulses, and the appearance of the emission seems quasi-periodic. The null fraction from the data is estimated to be 93.6%. No emission is detected in the integrated profile of all null pulses. Systematic modulations of pulse intensity and phase are found at the beginning of burst-pulse sequences just after null. The intensity usually rises to a maximum for the first few pulses, then declines exponentially afterwards, and becomes stable after few tens of pulse periods. The peak phase appears at later longitudes for the first pulse, then drifts to earlier longitudes rapidly, and then systematic drifting gradually vanishes while the intensity becomes stable. In this pulsar, the intensity variation and phase modulation of pulses are correlated in a short duration after the emission starts following a null. Observed properties of the pulsar are compared with other nulling pulsars published previously, and the possible explanation for phase modulation is discussed.

**Key words:** stars: neutron-pulsars: individual: nulling: PSR J1502–5653

## 1 INTRODUCTION

Pulsar nulling, which was first reported by Backer (1970), is a phenomenon in which the pulse emission abruptly turns off for a certain number of pulse periods, then suddenly returns to normal. Early studies showed that the “Nulling Fraction” (NF), i.e. the fraction of time that a pulsar is in null state, of most nulling pulsars is less than 10% (Biggs 1992; Vivekanand 1995). Wang et al. (2007) studied a sample of 23 nulling pulsars, including some extreme nulling pulsars with NF up to 95%.

Investigating the emission behaviors of nulling pulsars is important to understand the pulsar emission mechanism. Different patterns of transition between null and burst state have been noted by several authors. For PSR B1749–28 (Ritchings 1976), B0809+74 (Lyne & Ashworth 1983; van Leeuwen et al. 2003), B1944+17 (Ritchings 1976; Deich et al. 1986) and B0818–41 (Bhattacharyya et al. 2010), the onset of burst is abrupt, and the transition from burst to null state shows a gradual decline of pulse emission. However, the pulse intensity increases gradually when emission starts after a null for PSR J0941–39 (Burke-Spolaor & Bailes 2010), and the cessation of emis-

sion is sudden for PSR B0031–07 (Vivekanand 1995) and B0818–13 (Lyne & Ashworth 1983). Bhattacharyya et al. (2010) investigated the post- and pre-null emission behavior of PSR B0818–41, and showed that the first few pulses after the nulls outshine following pulses, whereas the last few pulses before the nulls are less intense than other pulses, and they noted that the phenomenon of null may be associated with some kind of ‘reset’ of the pulsar radio emission engine. Null of most pulsars occurs randomly. However, Kramer et al. (2006) reported the quasi-periodic nulls of B1931+24, furthermore, periodicity in nulling pulsars has been detected in PSR B1133+16 (Herfindal & Rankin 2007), J1819+1305 (Rankin & Wright 2008) and J1738–2330 (Gajjar et al. 2009).

PSR J1502–5653 was discovered during the Parkes Multibeam Pulsar Survey (Hobbs et al. 2004). The rotation period of the pulsar  $P$  is 0.535 s, and its first derivative  $\dot{P}$  is  $1.83 \times 10^{-15} \text{ s s}^{-1}$ . Correspondingly, it has a characteristic age of  $4.64 \times 10^6$  years and surface magnetic field strength of  $10^{12}$  gauss (Hobbs et al. 2004). Wang et al. (2007) investigated J1502–5653 at 1518 MHz and showed that this pulsar has a NF of 93%, which makes it an extreme nulling pulsar, with active pulses lasting typically a minute at intervals of 10 to 15 min of null pulses.

In this paper we carry out a detailed investigation of

\* E-mail: aliyi@xao.ac.cn

the emission behavior of PSR J1502–5653. Data analysis and results are presented in Section 2. The implications of the results are discussed in Section 3. Finally in Section 4, we summarize this work.

## 2 DATA ANALYSIS AND RESULTS

The data were obtained on September 12, 2002 using the Parkes 64-m telescope, at a central frequency of 1374 MHz. The data last for 6 hours, and contain 40308 pulse periods. The filterbank system has a total bandwidth of 288 MHz with  $96 \times 3\text{MHz}$  channels of polarization-summed data (for each beam) which are sampled every 1 ms. Details of the observing system are described by Manchester et al. (2001). The single-pulse time sequence is obtained by de-dispersing the data at a dispersion measure ( $DM$ ) of  $194.0 \text{ pc cm}^{-3}$ . Pulse intensities were computed by summing samples within an on-pulse window of width 20 ms and subtracting the baseline level determined in an off-pulse window of width 200 ms.

### 2.1 Time sequence and blocks of successive pulses

As shown in Fig. 1, the time sequence shows many blocks of consecutive strong pulses. In this paper, we considered intervals more than ten pulse periods with no detectable emission as null state, and intervals between null states as burst states. In this way, a total of 29 blocks of burst state (3451 pulses) are identified. The duration of these blocks varies from about 32 s (60 pulses) to 2 min (240 pulses), with an average duration of 1 min, while null state lasts from about 16 s (30 pulses) to 25 min (2800 pulses). The Fourier transformation of the autocorrelation function of the whole time sequence shows two relatively broad peaks at periods of 11 min and 18 min, implying the burst appearance of the pulsar may be quasi-periodic.

Ten typical blocks of burst are displayed in separate plots of Fig. 2 in the form of grayscale diagram (left panel) and intensity diagram (right panel). The burst blocks in these plots begin from the 11th pulse, and preceding 10 nulls are reserved for comparison. The first ten pulses in each block are quite strong, and the first few tens of pulses are uninterrupted by nulls. However, in the middle or late stages of some burst blocks, the pulse sequence is interrupted by a few short nulls, usually less than 10 periods. Just following some burst blocks, one or two sporadic strong pulses are detected occasionally during the null state. These sporadic single pulses are similar to the pulses during burst states in intensity, phase and shape.

As can be seen in Fig. 2, the pulse intensity shoots up to a relatively high magnitude for the first few pulses, and then the pulse intensity drops gradually. After about ten to twenty pulses, this relatively steady decrease is replaced by a pattern of random fluctuation in intensity. As shown in the left panel of Fig. 2, the single pulses drift from later to earlier longitudes at the beginning of each block of burst, and then present irregular modulation in pulse phase. These indicate that the variations of pulse intensity and pulse phase modulations may be correlated at the early stage of burst; this is studied further in Section 2.3. All the 29 blocks of

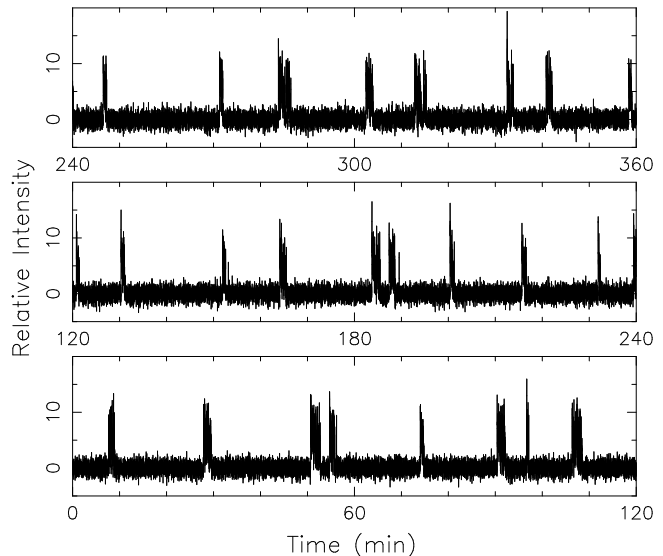


**Figure 1.** Six hours of time sequence of PSR J1502–5653. The time sequence is equally divided into three panels, each presents two hours of data.

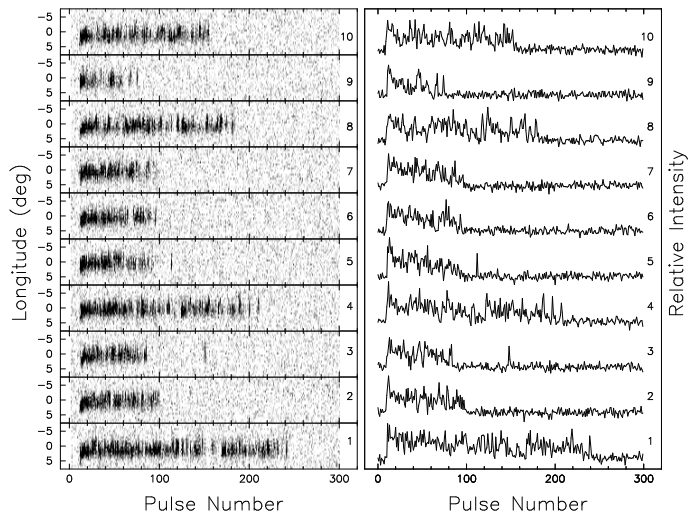


**Figure 2.** Ten blocks of 300 individual pulse periods containing burst presented in grayscale diagram (left panel) and intensity diagram (right panel) from PSR J1502–5653. Phase shifting to earlier longitude and intensity declining can be seen clearly at the early stage of each burst block.

burst start with abrupt rise of the intensity, and at least 23 of them end up with a gradual decline.

### 2.2 Average profiles and pulse energy distributions

Fig. 3 shows the integrated profiles for the whole data span including both burst and null pulses and for just the null pulses. There is no detectable profile by integrating all pulses in null state, whereas when the 3451 pulses in burst blocks added in, the profile is prominent showing that the burst pulses are actually very strong. The average profile of the pulsar is narrow, with a 10 per cent width of  $9.4^\circ$  (14 ms) in longitude.

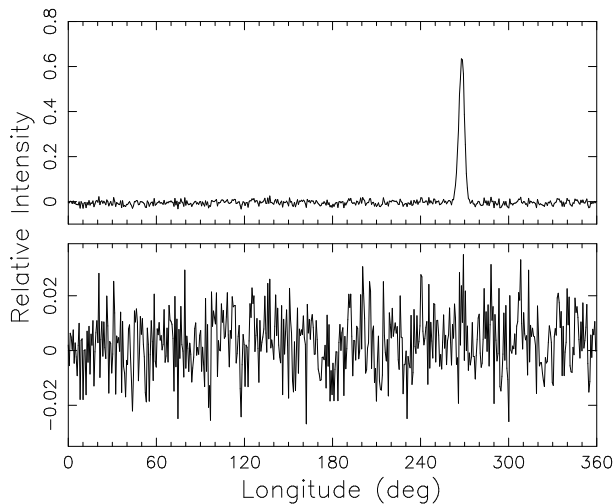


**Figure 3.** Integrated profiles of PSR J1502–5653 for all 40308 pulses (top panel) and the 36857 null pulses (bottom panel).

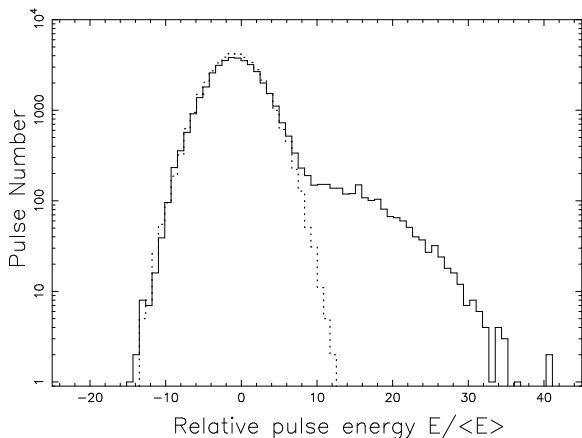


**Figure 4.** Histogram of on-pulse (solid line) and off-pulse (dotted line) energies normalized by the mean pulse energy for PSR J1502–5653.

Fig. 4 presents histograms of pulse energy distribution in the pulsar’s on-pulse and off-pulse windows, which are constructed using the method described by Ritchings (1976). On-pulse and off-pulse energies are determined by integrating within a on-pulse window and in a off-pulse window of same duration after a same baseline subtracted, respectively. The histogram formed from off-pulse energies (dot line) centers around zero, while that from on-pulse energies (solid line) have a “long tail” component due to burst pulses and a big gaussian component due to null pulses. The NF of the pulsar is estimated to be 93.6% through the histograms. As shown in this figure, the energy of the strongest pulse is 42 times that of mean pulse, suggesting the burst pulses are strong and highly modulated. This is the first pulse in the burst which situated at about 332 min in Fig. 1.

### 2.3 Single pulse intensity variation and phase modulation

To further study the emission behavior of PSR J1502–5653 during the early stage of burst just after null, we construct

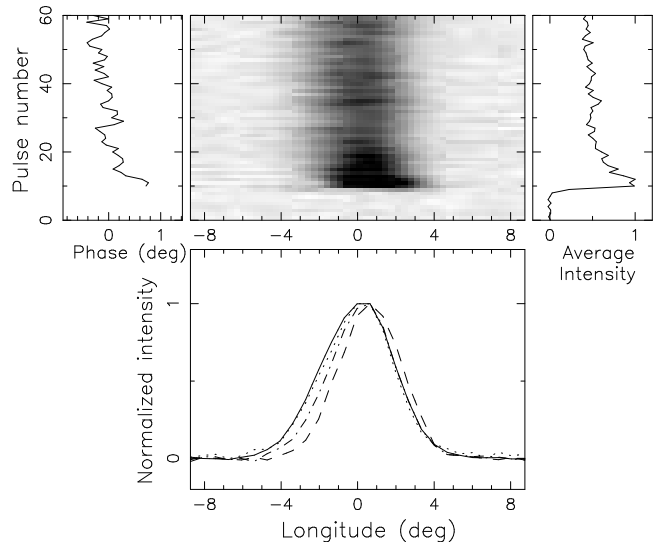


**Figure 5.** Phase and intensity variations of mean pulse sequence (see text). The top-middle panel shows gray-scale plot of the sequence. The top-left and top-right panel present phase and intensity variation of the mean pulse sequence respectively. The bottom panel shows the average profile (solid line) and three profiles, which are formed from the first three pulses (dashed line) in burst state, the fourth to ninth pulse (dot-dashed line) and the tenth to 15th pulse (dotted line), respectively.

the mean pulse sequence by superimposing the first 50 detectable burst pulses of all blocks (the shortest burst block contains more than 50 burst pulses) in accordance with the sequence of pulses and the pulse phases, while ten earlier pulses are also included for comparison. The distinguishable boundaries from null to burst, the abundance of burst blocks in the data and no null appears in the first 50 pulses in all burst blocks make this method feasible and effective in investigating the emission properties of the early stage of burst. The result is plotted in the top-middle panel of Fig. 5. The intensity fluctuation and phase modulation of the first ten pulses in the burst state look different from that of the following pulses.

As shown in the top-right panel of Fig. 5, the intensity shoots up at the first mean pulse in the burst state, and remains strong for about three pulses, then goes down exponentially for following sequence of about twenty pulses, and becomes stable at the half of maximum intensity for next tens of pulses. Using the method described by Bhattacharyya et al. (2010), we calculate that the average intensity of the first three mean pulses in the burst state is 1.4, 1.8, 2.2 and 2.4 times that of the following No. 4-9, 10-15, 31-40 and 41-50 mean pulses respectively.

The top-left panel of Fig. 5 shows that the peak phases of the first few burst pulses appear at later longitudes than that of the following pulses. In about thirteen pulse periods, the pulse phase drifts about 0.8 degree to earlier longitudes, and the phase of the 13th pulse is equal to the peak phase of average profile, then the apparent drifting stops and is replaced by irregular phase modulation. We note that the intensity fluctuation and phase modulation of the pulsar is correlated in the beginning of burst.

In Fig. 5 there is some evidence for a weak wide pulse at the start of burst. This pulse is the 10th pulse in the

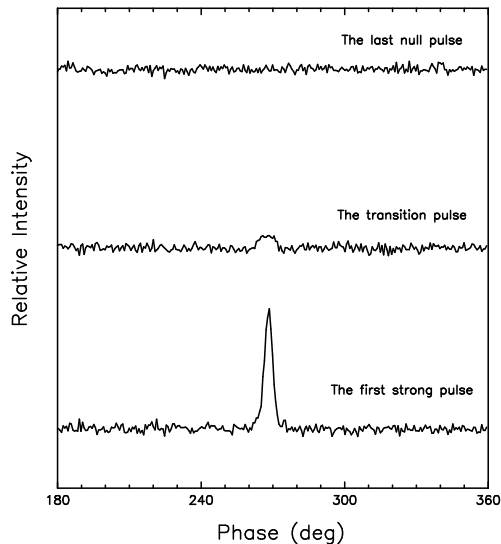


**Figure 6.** Plots of three consecutive pulses selected from the mean pulse sequence. From top to bottom, they are the 9th, 10th and 11th pulses in the mean pulse sequence. The top one is the last null pulse, the middle is the transition pulse at the start of burst and the bottom one corresponds to the first pulse after the transition pulse in the mean pulse sequence.

mean pulse sequence. We call it “transition pulse” in this paper. Fig. 6 shows three consecutive pulses selected from the mean pulse sequence, the last null pulse, the transition pulse, and the first strong pulse. The transition pulse have the full width at half maximum (FWHM) of  $6.7^\circ$  and signal-to-noise ratio (S/N) of 4.34. For comparison, the S/N of the first strong burst pulse is 44.1 and the width is  $4.04^\circ$ . The transition pulse is very weak, so it is only detectable in the mean pulse sequence.

The bottom panel in Fig. 5 displays the average profile (solid line) of the pulsar and three profiles which are obtained from the first three pulses following the transition pulse, the fourth to the ninth pulses and the tenth to 15th pulses, respectively. The peaks of these three profiles appear at longitudes  $0.72^\circ$ ,  $0.35^\circ$  and  $0.13^\circ$  respectively, where the peak phase of the average profile is set as zero. The widths of these three profiles are  $3.86^\circ$ ,  $4.06^\circ$  and  $4.33^\circ$ , respectively, while that of the average profile is  $4.53^\circ$ .

Fig. 7 presents the FWHM of **25** mean pulses in burst state, excluding the transition pulse, showing that the FWHM increases with pulse number at the beginning of burst. Around the 13th pulse of the burst the width reaches that of the average profile. Apart from the wide transition pulse, it is clear that in a short duration after the null, the radiation window gradually broadens while the pulses drift from later to earlier longitudes. The middle and later stage in burst block are often randomly disrupted by short nulls, and the behaviour is not so systematic as in the early stages.

### 3 DISCUSSION

The emission of J1502–5653 is characterized by abrupt transition from null to burst with a timescale of less than two pulse periods, a gradual decrease of pulse intensity in the early stage of a burst which is accompanied by a shift to

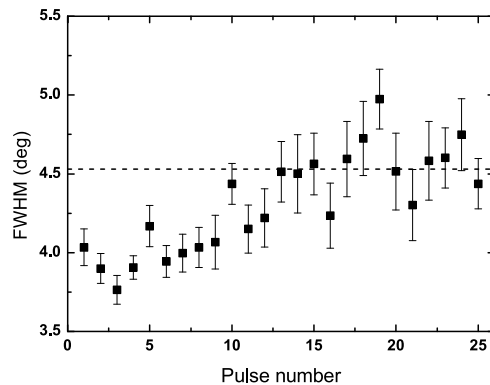


**Figure 7.** FWHM of the 25 mean pulses in burst state of the mean pulse sequence versus the corresponding pulse number. The dashed line denotes the pulse width of the average profile. The error of the width is derived from the uncertainty given by standard gaussian fitting procedure.

earlier longitude in pulse phase, and a broadening in pulse width. Gradual cessation of the emission in some bursts before nulls is also noticed. Similar behavior can be seen in PSR B0818–14. Bhattacharyya et al. (2010) reported that, for this pulsar, the transition from nulls to bursts is abrupt and pulse intensity from bursts to nulls appears to reduce gradually, and the profile shape of the first few pulses differs from that of average profile. They also mentioned that the behavior of subpulse drifting at the beginning of burst pulses after null is different from the following pulses. Similarly, in PSR J1502–5653, the pattern of phase modulation of the first few pulses is distinct from that of the later pulses during burst.

Recently, Burke-Spolaor & Bailes (2010) discovered bizarre emission behavior of PSR J0941–39, i.e. sometimes it only emits sporadic pulses and at other times it behaves just like a nulling pulsar. From Fig. 5 of Burke-Spolaor & Bailes (2010), we notice that the post-null pulse phases seem to shift towards earlier longitudes, and this looks similar to the drifting behavior of PSR J1502–5653. However, unlike PSR J1502–5653, the pulse intensity of PSR J0941–39 appears to increase gradually at the beginning of post-null emission, when it behaves like a nulling pulsar.

The post-null pulse drifting of PSR J1502–5653 may be explained by the vacuum gap model (Ruderman & Sutherland 1975). According to the classical vacuum gap model, the sub-beams of emission circulate around the magnetic axis, as a result of  $\mathbf{E} \times \mathbf{B}$  drift of spark plasma filaments. At the beginning of each burst, the electric field in the accelerating gap is relatively high and in consequence the observed  $\mathbf{E} \times \mathbf{B}$  drift-rate is high. Then the sparking process starts, which produces not only strong radio emission but also  $e^+ e^-$  pairs. Few pulses periods later, the  $e^+ e^-$  pairs accumulate in the accelerating gap and decrease the electric field to a relatively stable value where sparking and radio emission go on but the drift-rate reduces to nearly zero. As the accumulation proceeds the gap electric field strength keeps on weakening until sparking process breaks down and the radio emission ceases. Gil et al. (2003, 2008) refined the vacuum model by introducing a thermal ion outflow from the hot polar

cap surface. However, the intensity variations and their correlation with phase modulation of burst pulses at the beginning of burst blocks need to be further investigated.

Kramer et al. (2006) noted that PSR B1931+24 turns ‘on’ for 5–10 days and ‘off’ for 25–35 days, the switch occurs in a quasi-periodic fashion, and no obvious emission can be found in the integrated profile of null state. The difference of the slow-down rates in the ‘on’ and ‘off’ states of this pulsar indicates a massive change in magnetospheric currents. The quasi-periodic transition between ‘on’ and ‘off’ state and non-detection of integrated energy by folding many null pulses of PSR J1502–5653, suggest that the emission behavior of this pulsar is somehow similar to that of the intermittent pulsar B1931+24, but with very different ‘on’ and ‘off’ timescales. The scenario of two slow-down rates of PSR B1931+24 may be applicable to PSR J1502–5653, however, measuring two slow-down rates is not possible for this pulsar, because of the very short durations of ‘on’ and ‘off’ states. The timescale of the magnetospheric-current changing is believed to be very short, and it is not yet clear whether and how the pulses emitted at the very beginning of strong burst state are influenced by the switching process of the magnetospheric currents.

#### 4 CONCLUSION

The bursts of pulses of PSR J1502–5653 have a typical duration of 1 min or about 100 pulse periods, and they are separated by nulls lasting from 30 to 2800 pulse periods. The power spectra of pulse sequence shows two broad peaks at periods of 11 min and 18 min, revealing that the appearance of the emission may be quasi-periodical in this pulsar. The nulling fraction estimated from the data is 93.6%. The integrated profile of all null pulses shows no emission. Interestingly, by integrating over 29 pulse sequences, a weak and wide pulse is found just before the first detected single pulse in all burst blocks.

At the beginning of burst after null the intensity usually rises to the maximum immediately, and keeps a high intensity for few pulses, then the intensity of next twenty or thirty pulses declines exponentially, and gradually becomes stable at the half of the maximum intensity. In most case, the cessation of radiation is gradual. The peak phase of the first pulse in burst usually appears to be at later longitudes than that of average profile, then the phase drifts quickly to earlier longitudes for next several pulses. The drifting then tends to slow down in next twenty to thirty pulse periods, and then is replaced by irregular phase modulation. As the peak phase drifts to earlier longitudes, the pulse intensity declines, meanwhile, the radiation window broadens gradually till reaching the width of average profile. A good correlation can be seen between intensity variation and phase modulation in the early stage of post-null emission.

The phase modulation may be explained by electric field shielding caused by  $e^+ e^-$  pairs produced by sparking process. The emission behaviors of individual pulses during the transition between null and burst state may provide very important clue to understand the underlying switching mechanism of nulling pulsars.

#### ACKNOWLEDGMENTS

This work was funded by the National Natural Science Foundation of China (NSFC) under No.10973026. We thank members of the Pulsar Group at XAO for helpful discussions. The Parkes radio telescope is part of the Australia Telescope which is funded by the Commonwealth Government for operation as a National Facility managed by the Commonwealth Scientific and Industrial Research Organization.

#### REFERENCES

- Backer D. C., 1970, *Nature*, 228, 42  
 Bhattacharyya B., Gupta Y., Gil J., 2010, *MNRAS*, 408, 407  
 Biggs J. D., 1992, *ApJ*, 394, 574  
 Burke-Spolaor S., Bailes M., 2010, *MNRAS*, 402, 855  
 Deich W. T. S., Cordes J. M., Hankins T. H., Rankin J. M., 1986, *ApJ*, 300, 540  
 Gajjar V., Joshi B. C., Kramer M., 2009, in D. J. Saikia, D. A. Green, Y. Gupta, & T. Venturi ed., *The Low-Frequency Radio Universe Vol. 407 of Astronomical Society of the Pacific Conference Series, Peculiar Nulling in PSR J1738-2330*. p. 304  
 Gil J., Haberl F., Melikidze G., Geppert U., Zhang B., Melikidze Jr. G., 2008, *ApJ*, 686, 497  
 Gil J., Melikidze G. I., Geppert U., 2003, *A&A*, 407, 315  
 Herfindal J. L., Rankin J. M., 2007, *MNRAS*, 380, 430  
 Hobbs G., Faulkner A., Stairs I. H., Camilo F., Manchester R. N., Lyne A. G., Kramer M., D’Amico N., Kaspi V. M., Possenti A., McLaughlin M. A., Lorimer D. R., Burgay M., Joshi B. C., Crawford F., 2004, *MNRAS*, 352, 1439  
 Kramer M., Lyne A. G., O’Brien J. T., Jordan C. A., Lorimer D. R., 2006, *Science*, 312, 549  
 Lyne A. G., Ashworth M., 1983, *MNRAS*, 204, 519  
 Manchester R. N., Lyne A. G., Camilo F., Bell J. F., Kaspi V. M., D’Amico N., McKay N. P. F., Crawford F., Stairs I. H., Possenti A., Morris D. J., Sheppard D. C., 2001, *MNRAS*, 328, 17  
 Rankin J. M., Wright G. A. E., 2008, *MNRAS*, 385, 1923  
 Ritchings R. T., 1976, *MNRAS*, 176, 249  
 Ruderman M. A., Sutherland P. G., 1975, *ApJ*, 196, 51  
 van Leeuwen A. G. J., Stappers B. W., Ramachandran R., Rankin J. M., 2003, *A&A*, 399, 223  
 Vivekanand M., 1995, *mnras*, 274, 785  
 Wang N., Manchester R. N., Johnston S., 2007, *MNRAS*, 377, 1383